RSC Advances

PAPER

View Article Online
View Journal | View Issue

Cite this: *RSC Adv.*, 2024, **14**, 23505

Polyfluorene–poly(ethylene oxide) diblock copolymers: synthesis and electron transport behavior†

Jin Cheng,[abc] Ruoyu Jiang,[ac] Yuhua Shan,[b] Hong Sun,[d] Shinji Kanehashi[ce] and Kenji Ogino*[ce]

Received 17th May 2024
Accepted 8th July 2024

DOI: 10.1039/d4ra03606a

rsc.li/rsc-advances

Under mild reaction conditions, we synthesized diblock copolymers of poly(9,9-dioctylfluorene)-*block*-poly(ethylene oxide) (**PFO-*b*-PEO**) *via* end-capping poly(9,9-dioctylfluorene) (PFO) with poly(ethylene oxide) (PEO) on one end. We investigated the thermal, optical, electrochemical and crystalline properties as well as electron transport performance of these polymers. Our results demonstrate that **PFO-*b*-PEO** diblock copolymers with short PEO chains (M_n = 1000 and 2000 g mol^{-1}) exhibit higher electron mobilities compared to the PFO homopolymer and longer PEO chain (M_n = 4000 g mol^{-1}) attached copolymers. This enhanced electron mobility is attributed to the higher crystallinity induced by the shorter PEO chain end-capping.

Introduction

As one of the promising polymers for light-emitting diode materials, polyfluorene exhibits superior processability, high photoluminescence quantum efficiency, and satisfactory stabilities in both thermal and electrochemical detection.[1,2] However, it expresses insufficient color stability, attributed to aggregates/excimers, interchain inter-actions, and/or emissive keto defects generated by troublesome thermo-, photo-, or electro-oxidative degradation during device operation.[3–8] Moreover, another severe problem for polyfluorene is poor electroluminescence (EL) efficiency associated with electron traps, which induces hole–electron transporting imbalance and Shockley–Read–Hall (SRH) trap-assisted recombination between trapped electrons and free holes.[9,10]

To suppress these adverse effects, decoration of the polyfluorene backbone, such as an alkyl/phenyl structure introduced at methylene bridged hydrogen,[11,12] functional groups attached as endcaps,[13–17] and elimination of adverse impact from electron traps *via* dilution of electron trap or the formation of more regular morphology or phase.[18–21]

Poly(9,9-dioctylfluorene) (PFO), as a polyfluorene derivative, with octyl groups in 9 active positions as side chains, was reported to induce good solubility and β-phase formation.[20,22]

As either an additive or an attached building block,[23–26] poly(ethylene oxide) (PEO) was widely chosen for its superior viscoelastic properties, which are well suited for improving the morphology of conjugated polymers. Previously, we synthesised a diblock copolymer of P3HT by incorporating PEO, which induced micro-phase separation and enhanced charge mobility.[27] This technique inspired us to assemble PEO into block copolymer architectures through chain elongation from terminals of the other polymer.

We synthesized PFO and PEO diblock copolymers for a luminescent material in electron-only (EO) devices. PEO segments were introduced at the terminals of PFO *via* the Steglich coupling reaction. Gel permeation chromatography (GPC) and ^{1}H-NMR were used to characterize the structures of the PFO homo-polymer and block copolymers. The thermal, optical, electrochemical, and crystalline properties of the polymers and the performances of the corresponding EO devices were examined.

Experimental

Materials

We prepared 2-(7-bromo-9,9-dioctyl-fluoren-2-yl)-4,4,5,5-tetramethyl-1,3,2-dioxaborolane (**1**) and 2-(4-iodophenoxy)-1-[*tert*-butyldimethylsiloxy]ethane (**2**) as reported in the literature.[28,29] Dry tetrahydrofuran (THF) and other reagents were obtained as commercial products and used without further

[a]*Department of Chemical Engineering and Pharmaceutical Engineering, Changzhou Vocational Institute of Engineering, Changzhou 213164, China. E-mail: chengjin82@163.com*

[b]*Jiangsu Province Key Laboratory of Fine Petrochemical Engineering, Changzhou University, Changzhou 213164, China*

[c]*Graduate School of Bio-Applications and Systems Engineering, Tokyo University of Agriculture and Technology, 2-24-16 Nakacho, Koganei-shi, Tokyo 184-8588, Japan. E-mail: kogino@cc.tuat.ac.jp*

[d]*Zhejiang Fenghong New-material Co. Ltd., Huzhou 313300, China*

[e]*Institute of Global Innovation Research, Tokyo University of Agriculture and Technology, 2-24-16 Nakacho, Koganei-shi, Tokyo 184-8588, Japan*

† Electronic supplementary information (ESI) available. See DOI: https://doi.org/10.1039/d4ra03606a

Table 1 Characteristics of PFO-2 and PFO-*b*-PEOs

Polymer	$M_{n,PEO\text{-}section}$[b] (g mol^{-1})	$M_{n,PFO\text{-}b\text{-}PEO}$ (g mol^{-1})		PDI[a]	PEO[b] (wt%)	Yields
PFO-2	—	9231[a]	8697[b]	2.22	—	80%
PFO-*b*-PEO1	975	10 552[a]	9568[b]	2.15	3.7	73%
PFO-*b*-PEO2	1914	10 966[a]	10 009[b]	3.10	6.4	63%
PFO-*b*-PEO4	3135	11 543[a]	12 059[b]	4.31	15.3	55%

[a] Determined *via* GPC. [b] Determined *via* ^{1}H-NMR.

purification. α-Monocarboxylic-ω-monomethoxy poly(ethylene oxide)s (PEO–COOHs), with number-average molecular weights (M_n) of 1000, 2000, and 4000, were synthesized according to an established procedure.[15]

Synthesis of hydroxyl end-functionalized polyfluorene (PFO-2)

Compound 1 (1.77 g) and deoxidized toluene (17 mL) were added to a 100 mL flask, and oxygen was removed *via* three freeze-and-thaw cycles with liquid nitrogen bath. Subsequently, to the mixture, 2 N K_2CO_3 (30 mL) (after 0.5 h nitrogen bubbling), compound 2 (35.4 mg), and $Pd(PPh_3)_4$(0) (37 mg) were added and deoxygenated *via* another three freeze-and-thaw cycles. The mixture was stirred at 90 °C under nitrogen for 24 h. After the reaction, we added chloroform (100 mL) at room temperature and then washed the mixture with brine thrice. After drying with $MgSO_4$, filtration, concentration, and reprecipitation in methanol, we obtained 0.99 g yellow solid product *tert*-butyldimethylsiloxyethoxy end-capped PFO (**PFO-1**).

The prepared **PFO-1** (0.99 g) was dissolved in dry THF (50 mL), and then HF/pyridine (0.36 mL) was dropwise added under nitrogen. The mixture was stirred at room temperature for 24 h. Following concentration and reprecipitation in methanol, we obtained 0.80 g of the yellow solid product **PFO-2** (yield: 80%).

Synthesis of PFO-*b*-PEO

PFO-2 (0.5 g, 0.05 mmol), PEO–COOH (0.5 mmol), dicyclohexylcarbodiimide (DCC) (1.78 g, 8.6 mmol), and 4-dimethylaminopyridine (DMAP) (1.06 g, 8.6 mmol) and dry dichloromethane (60 mL) were placed under nitrogen in a 100 mL flask. The mixture was then stirred at room temperature for 24 h. The resulting solution was evaporated to remove the solvent, and the residue was crushed with acetone (60 mL) by stirring overnight. Then, *via* Soxhlet extraction of the filtrated solid with acetone for 48 h, we produced the final lime solid **PFO-*b*-PEO** samples. Characteristics of **PFO-2** and **PFO-*b*-PEO**s are listed in Table 1.

Characterizations

^{1}H-NMR spectra were obtained on a JEOL ALPHA300 instrument at 300 MHz and 25 °C. Deuterated chloroform was used as a solvent with tetramethyl silane as an internal standard.

M_n and polydispersity index (PDI) was determined by gel permeation chromatography (GPC) analysis with a JASCO RI-2031 detector and eluted with chloroform at a flow rate of 0.5 mL min^{-1} at room temperature and calibrated by standard polystyrene samples.

The polymers' glass transition temperature (T_g) was measured by differential scanning calorimetry (DSC) analysis performed on a Rigaku DSC-8230 under a nitrogen atmosphere at heating and cooling rates of 10 °C min^{-1}.

Ultraviolet-visible (UV-vis) absorption spectra were obtained on the JASCO V-570 spectrophotometer, and photoluminescence (PL) spectra were detected on the JASCO FP-6500 spectrophotometer with an excitation at 380 nm. The films were formed in 2.5 cm × 2.5 cm glass plates. The polymer layer was laminated by spin-coating at 1000 rpm for 60 s from chlorobenzene solution (40 mg mL^{-1}) filtered using a 0.45 mm membrane filter. The procedure of film fabrication was almost the same as for EO devices on ITO substrates.

Cyclic voltammetry (CV) was conducted on a Niko Keisoku Model NPGFZ-2501-A Potentiostat/Galvanostat. All measurements were carried out at room temperature in a typical three-electrode cell with a working electrode (glassy carbon electrode), a reference electrode (Ag/AgCl), and a counter electrode (Pt wire) at a scanning rate of 0.1 V s^{-1}. All measurements were performed using acetonitrile and tetrabutylammonium tetrafluoroborate (Bu_4NBF_4) (0.1 M) as solvents and supporting electrolytes, respectively.

The crystal structure of the films on the glass was measured by grazing incidence wide-angle X-ray diffraction (GIWAXD) (RIGAKU X-ray Diffractometer SmartLab) (Cu Kα, $\lambda = 1.5418$ Å, 45 kV, and 200 mA) from 3° to 30° with a step of 0.02° at the scan speed of 1° min^{-1} in the out-of-plane measurements. The incident angle was fixed at 0.14°. The thickness of the films and metals was measured using a Stylus-type surface profiler (BRUKER, Dektak XT-S).

Results and discussion

Synthesis and characterization

As shown in Scheme 1, we synthesized *tert*-butyldimethylsiloxyethoxy end-capped **PFO-1** *via* the Suzuki–Miyaura reaction, and by following deprotection of *tert*-butyldimethylsiloxyethoxy with

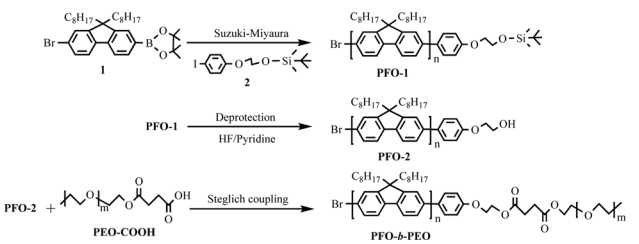

Scheme 1 Synthesis route.

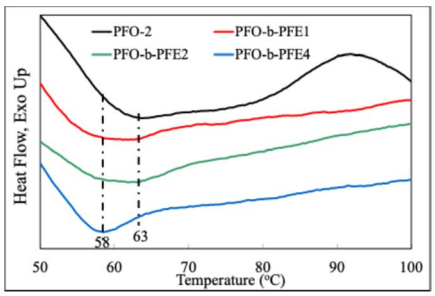

Fig. 1 DSC thermograms for PFO-2 and PFO-*b*-PEOs.

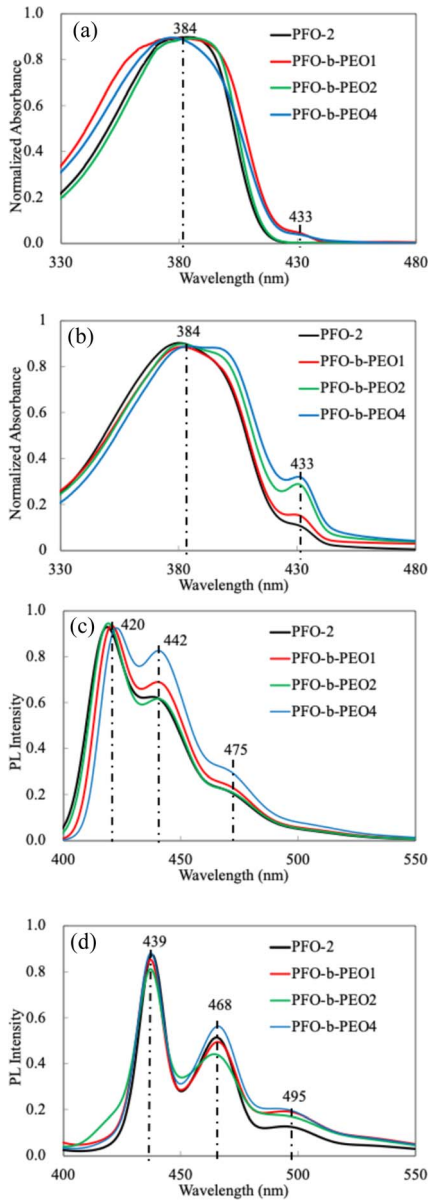

Fig. 2 UV-vis and PL spectra of PFO-2 and PFO-*b*-PEOs: (a) UV-vis, solution, (b) UV-vis, film, (c) PL, solution, and (d) PL, film.

HF/pyridine, **PFO-2** was produced with low steric hindrance $PhOCH_2CH_2OH$ terminating group. **PFO-2** and PEO–COOH were then linked to form diblock copolymer **PFO-*b*-PEO** *via* a mild Steglich coupling reaction (room temperature, 24 h). The key factor that influences the Steglich coupling reaction for the formation of **PFO-*b*-PEO**s is the low steric hindrance of the hydroxyl group on **PFO-2** and the carboxyl group on PEO. This low steric hindrance is crucial as it allows the functional groups to react more readily, minimizing spatial barriers and facilitating efficient coupling.

Table 2 Optical and electrochemical properties of PFO-2 and PFO-*b*-PEOs

Polymer	λ_{max} (nm), film	E_{red} (V)	E_{LUMO}[a] (−eV)
PFO-2	383, 433	−0.74	3.66
PFO-*b*-PEO1	383, 433	−0.74	3.66
PFO-*b*-PEO2	384, 433	−0.73	3.67
PFO-*b*-PEO4	384, 433	−0.74	3.66

[a] $E_{LUMO} = -(E_{red} + 4.4)$ (eV).

By employing different M_n PEO–COOHs, we successfully obtained a series of diblock copolymers with different PEO weight content (shown in Table 1). The PDI of the **PFO-*b*-PEO4** was significantly larger compared to other polymers. This can be attributed to the increased crystallinity of longer PEO chains. As the M_n of the PEO segments increases (*e.g.*, M_n = 4000 g mol^{-1}), their crystallinity is enhanced, leading to stronger interchain interactions and a broader PDI.[30]

Thermal properties

As depicted in Fig. 1, homopolymer (**PFO-2**) showed an endothermic peak around 63 °C, attributed mainly to the melting of the conjugated PFO backbone. The curves of diblock copolymers (**PFO-*b*-PEO1** and **PFO-*b*-PEO2**) revealed double endothermic peaks near 58 C° and 63 °C, and the newly emerging rise might be related to the melting of the PEO chains. In the curve of PFO-*b*-PFE4, the peak around 63 °C became not obvious; we attributed it to the large-scale crystallization of longer PEO chains, which might inhibit the crystallization of the conjugated PFO backbone. This fact also echoes the previous discussion on the impact of long-chain PEO on PDI.

Optical properties

As shown in Fig. 2 and Table 2, the UV-vis spectra of all homo- and diblock copolymers demonstrated similar λ_{max} around 384 nm in both states. In addition, all polymers expressed similar redshift at about 433 nm in Fig. 2b, owing to the β-phase formation in the film state. It is reported that the β-phase formation is related to a series of attractive features in PLED, such as higher carrier mobility, higher current efficiency, and excellent spectral stability.[31]

From Fig. 2a and b, we observed an increase in the β-phase composition with higher M_n PEO segments. This phenomenon can be attributed to reduced chain mobility. Longer PEO chains decrease the mobility of polymer chains through entanglements and enhance the intermolecular interactions, thereby promoting the formation of the stable β-phase conformation in PFO chains.[32]

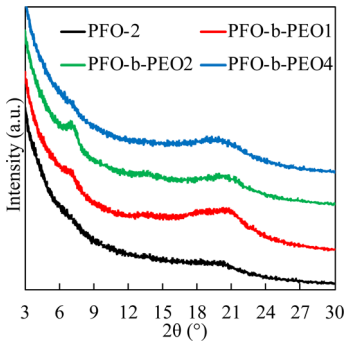

Fig. 3 GIWAXD profiles obtained with out-of-plane geometry for thin films of PFO and **PFO-*b*-PEO**s fabricated with chlorobenzene.

On the other hand, all polymers exhibited similar PL spectra in both solution and film states. This indicates that incorporating PEO as a block segment exerts minimal impact on the PL properties of PFO. The PL spectra of all the polymers showed a primary emission peak at around 420 nm in the solution and 439 nm in the film, a shoulder peak approximately at 442 nm in the solution and 468 nm in the film, and a long-wavelength emission peak around 475 nm in the solution and 495 nm in film; these peaks correspond to the π–π* transitions within the polyfluorene molecules, the microstructural features of the polyfluorene chains, and additional microstructural characteristics of the polyfluorene chains, respectively.[33,34]

Electrochemical properties

The electrochemical properties of the polymers were investigated by CV, as shown in Table 2; the reduction process of **PFO-2** and **PFO-*b*-PEO**s started at about −0.74 V, and LUMO levels of all polymers were calculated to be about −3.66 eV, indicating that the PEO block section has little effect on the LUMO levels of PFO polymer.

Crystalline structure analysis

As shown in Fig. 3, stronger peaks appeared in the diblock copolymers curves at *ca.* $2\theta \approx 20°$, corresponding to π–π stacking distances of 4.2–4.4 Å, exhibiting crystalline patterns with distinct diffraction peaks.[35,36] In the case of **PFO-2**, the rise was relatively weaker, implying a nearly non-crystalline (amorphous) profile. The same result was observed at $2\theta \approx 7.5°$, corresponding to lamellar patterned *d*-spacings.[37]

Furthermore, we found that both peaks at *ca.* $2\theta \approx 20°$ and $2\theta \approx 7.5°$ were stronger in **PFO-*b*-PEO1** and **PFO-*b*-PEO2** than in PFO-*b*-PFO4, indicating the inhibition of the crystallite formation in the presence of overlong PEO chains, echoing the results of the thermal properties we discussed.

Electron transporting properties

The performance of the EO devices based on **PFO-2** homopolymer and **PFO-*b*-PEO** block copolymers with the configuration of ITO/Al/polymer/LiF/Al was evaluated. Electron mobility in the space-charge-limited current, the SCLC region was determined

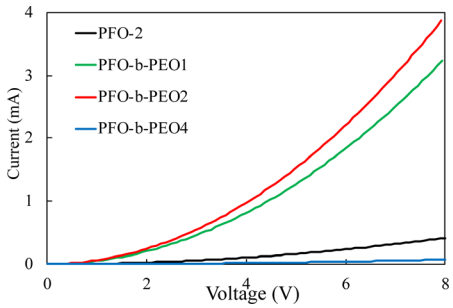

Fig. 4 Current–voltage characteristics of EO devices based on **PFO-2** and **PFO-*b*-PEO**s.

Table 3 Electron mobility($cm^2\ V^{-1}\ s^{-1}$) of **PFO-2** and **PFO-*b*-PEO**s

Polymer	Electron mobility[a] ($cm^2\ V^{-1}\ s^{-1}$)
PFO-2	4.5×10^{-7}
PFO-*b*-PEO1	3.3×10^{-6}
PFO-*b*-PEO2	3.9×10^{-6}
PFO-*b*-PEO4	1.1×10^{-7}

[a] Average values determined for four devices.

from the *I–V* characteristic curves utilizing the following eqn (1), taking the series resistance (12 Ω) into consideration and assuming that the built-in voltage was close to zero due to the slight difference of work functions for both electrodes.[38]

$$J = \frac{9}{8}\varepsilon_r\varepsilon_0\mu_e\frac{V^2}{L^3} \quad (1)$$

where J is the electron current density, μ_e is the electron mobility, ε_r is the relative permittivity of the material (3.5), ε_0 is the permittivity of vacuum, L is the thickness of the active layer, and V is the voltage drop across the device.

The electron mobilities of devices fabricated from **PFO-2** and **PFO-*b*-PEO**s are shown in Fig. 4 and Table 3. **PFO-*b*-PEO1** and **PFO-*b*-PEO2** exhibited higher electron mobility than **PFO-2** and **PFO-*b*-PEO4**. Since they had similar performances in optical and electrochemical properties, we owed this enhancement to the fact that a short PEO polymer chain block section can improve the crystalline properties of PFO.

Conclusions

In summary, we successfully synthesized **PFO-*b*-PEO**s using a mild Steglich coupling reaction. The investigation of these copolymers revealed their potential to enhance the electron transport properties, with particular improvements noted in the materials with shorter PEO chain segments. This work highlights the significant impact of chain length and structural modifications on the properties of **PFO-*b*-PEO** copolymers.

Future studies should focus on further exploring the relationship between the molecular architecture of **PFO-*b*-PEO** copolymers and their electronic properties. Additionally, there is considerable potential in investigating the application of these materials in various optoelectronic devices, such as

organic photovoltaics (OPVs) and field-effect transistors (FETs). Understanding the detailed mechanisms of electron transport and phase behavior in these copolymers could lead to the development of more efficient and stable electronic materials.

Data availability

^{1}H-NMR spectra of **PFO-1**, **PFO-2**, **PFO-*b*-PEO1**, **PFO-*b*-PEO2**, and **PFO-*b*-PEO4** are available in the ESI (https://doi.org/10.1039/d4ra03606a). Fig. S1: ^{1}H-NMR spectra of **PFO-1** in $CDCl_3$ at 300 MHz; Fig. S2: ^{1}H-NMR spectra of **PFO-2** in $CDCl_3$ at 300 MHz; Fig. S3: ^{1}H-NMR spectra of **PFO-*b*-PEO1** in $CDCl_3$ at 300 MHz; Fig. S4: ^{1}H-NMR spectra of **PFO-*b*-PEO2** in $CDCl_3$ at 300 MHz; Fig. S5: ^{1}H NMR spectra of **PFO-*b*-PEO4** in $CDCl_3$ at 300 MHz.†

Author contributions

Jin Cheng and Kenji Ogino conceived and designed the experiments; Jin Cheng performed the experiments; Jin Cheng, Ruoyu Jiang, and Kenji Ogino analyzed the data; Jin Cheng wrote the main bulk of the article; Yuhua Shan, Hong Sun, and Kenji Ogino improved and finalized the article; Yuhua Shan, Shinji Kanehashi and Kenji Ogino contributed reagents/materials/analysis tools.

Conflicts of interest

The authors declare no conflict of interest.

Acknowledgements

This research was funded by the "Jiangsu Province Key Laboratory of Fine Petrochemical Engineering, grant number KF2023." and the "Grant-in-Aid for Scientific Research from the Japan Society for the Promotion of Science (JSPS), KAKENHI, grant number (15K05661)".

Notes and references

1 C. A. Young, A. Hammack, H. J. Lee, H. Jia, T. Yu, M. D. Marquez, A. C. Jamison, B. E. Gnade and T. R. Lee, *ACS Omega*, 2019, **27**, 22332.
2 G. Sardar, A. Shukla, E. G. Moore, G. Banappanavar, S. Lo, E. B. Namdas and D. Kabra, *J. Phys. Chem. C*, 2022, **126**, 9069.
3 E. J. W. List, R. Guentner, P. S. de Freitas and U. Scherf, *Adv. Mater.*, 2002, **911**, 734.
4 L. Romaner, A. Pogantsch, P. S. de Freitas, U. Scherf, M. Gaal, E. Zojer and E. J. W. List, *Adv. Funct. Mater.*, 2003, **13**, 597.
5 J. K. Jin, S. K. Kwon and Y. H. Kim, *Macromolecules*, 2009, **42**, 6339.
6 A. Bolognesi, P. Betti, C. Botta and S. Destri, *Macromolecules*, 2009, **42**, 1107.
7 M. Kreyenschmidt, G. Klarner, T. Fuhrer, J. Ashenhurst, S. Karg, W. D. Chen, V. Y. Lee, J. C. Scott and R. D. Miller, *Macromolecules*, 1998, **31**, 1099.
8 J. I. Lee, G. Klarner and R. D. Miller, *Chem. Mater.*, 1999, **11**, 1083.
9 X. Gong, P. K. Iyer, D. Moses, G. C. Bazan, A. J. Heeger and S. S. Xiao, *Adv. Funct. Mater.*, 2003, **13**, 325.
10 G. Klarner, J. I. Lee, V. Y. Lee, E. Chan, J. P. Chen, A. Nelson, D. Markiewicz, R. Siemens, J. C. Scott and R. D. Miller, *Chem. Mater.*, 1999, **11**, 1800.
11 Q. S. Zhang, *Chin. J. Chem.*, 2010, **28**, 1482.
12 S. K. Lee, T. Ahn and N. S. Cho, *J. Polym. Sci., Part A: Polym. Chem.*, 2007, **45**, 1199.
13 H. Hsieh, C. Hung, K. Watanabe, J. Chen, Y. Chiu, T. Isono, Y. Chiang, R. R. Reghu, T. Satoh and W. Chen, *Polym. Chem.*, 2018, **9**, 3820.
14 L. Verheyen, K. Janssens, M. Marinelli, E. Salatelli and G. Koeckelberghs, *Macromolecules*, 2019, **52**, 6578.
15 H. H. Ahn, S. H. Jang, B. Hwang, J. Yoon, S. Y. Kim, S. J. Noh, J. Y. Han and Y. K. Kwon, *Polymer*, 2013, **54**, 4864.
16 Y. Tan, Z. Gu, K. Tsuchiya and K. Ogino, *Polymer*, 2012, **53**, 1444.
17 K. Saito, T. Isono, H. Sun, T. Kakuchi, W. Chen and T. Satoh, *Polym. Chem.*, 2015, **6**, 6959.
18 A. Kunz, P. W. M. Bloma and J. J. Michels, *J. Mater. Chem. C*, 2017, **5**, 3042.
19 E. Khodabakhshi, P. W. M. Blom and J. J. Michels, *Appl. Phys. Lett.*, 2019, **114**, 093301.
20 D. W. Bright, F. B. Dias, F. Galbrecht, U. Scherf and A. P. Monkman, *Adv. Funct. Mater.*, 2009, **19**, 67.
21 W. Zhu, C. Wei, X. An, J. Weng, B. Liu, N. Wang, N. Sun, L. Sun, M. Yu, J. Lin, L. Bai, C. Sun, D. Lu, L. Xie and W. Huang, *ACS Appl. Polym. Mater.*, 2019, **1**, 2352.
22 P. Wilhelm, D. Blank, J. M. Lupton and J. Vogelsang, *ChemPhysChem*, 2020, **21**, 1.
23 C. H. Lyons, E. D. Abbas, J.-K. Lee and M. F. Rubner, *J. Am. Chem. Soc.*, 1998, **120**, 12100.
24 S. Chien, F. Chen, M. Chung and C. Hsu, *J. Phys. Chem. C*, 2012, **116**, 1354.
25 Y. Honmou, S. Hirata, H. Komiyama, J. Hiyoshi, S. Kawauchi, T. Iyoda and M. Vacha, *Nat. Commun.*, 2014, **5**, 4666.
26 A. B. Schantz, P. O. Saboe, I. T. Sines, H.-Y. Lee, K. J. M. Bishop, J. K. Maranas, P. D. Butler and M. Kumar, *Macromolecules*, 2017, **50**, 2484.
27 K. Hayashi, K. Kanehashi and K. Ogino, Structural Analysis of Poly(3-Hexylthiophene)-*b*-Poly(ethylene Oxide) and Evaluation of Hole Mobility, *Autumn Research Conference of the Society of Fiber Science and Technology*, Nagano, Japan, 2019.
28 X. Zhang, H. Tian, Q. Liu, L. Wang, Y. Geng and F. Wang, *J. Org. Chem.*, 2006, **71**, 4332.
29 B. Malo-Forest, G. Landelle, J. Roy, J. Lacroix, R. C. Gaudreault and J. Paquin, *Bioorg. Med. Chem. Lett.*, 2013, **23**, 1712.
30 H. Feng, X. Lu, W. Wang, N.-G. Kang and J. W. Mays, *Polymers*, 2017, **9**, 494.
31 X. Zhang, Q. Hu, J. Lin, Z. Lei, X. Guo, L. Xie, W. Lai and W. Huang, *Appl. Phys. Lett.*, 2013, **103**, 153301.

32 N. Golzari, J. Adams and S. Beuermann, *Polymers*, 2017, **9**, 306.
33 Q. Zhang, P. Wang, G. L. Ong, S. H. Tan, Z. W. Tan, Y. H. Hii, Y. L. Wong, K. S. Cheah, S. L. Yap, T. S. Ong, T. Y. Tou, C. H. Nee, D. J. Liaw and S. S. Yap, *Polymers*, 2019, **11**, 840.
34 H. T. Kidanu, J. H. Lee and C. Chen, *Mater. Adv.*, 2021, **2**, 3589.
35 E. Lim, B. J. Jung, J. Lee, H. K. Shim, J. I. Lee, Y. S. Yang and L. M. Do, *Macromolecules*, 2005, **38**, 4531.
36 Y. Wu, Y. Li, S. Gardner and B. S. J. Ong, *J. Am. Chem. Soc.*, 2005, **127**, 614.
37 S. Hayashi, S. Inagi and T. Fuchigami, *Polym. J.*, 2010, **42**, 772.
38 C. R. Singh, G. Gupta, R. Lohwasser, S. Engmann, J. Balko, M. Thelakkat, T. Thurn-Albrecht and H. Hoppe, *J. Polym. Sci., Part B: Polym. Phys.*, 2013, **51**, 943.